Eur. Phys. J. C 39, 195–200 (2005)
Digital Object Identifier (DOI) 10.1140/epjc/s2004-02086-9

THE EUROPEAN PHYSICAL JOURNAL C

Spectrum of recoil nucleons in quasi-elastic neutrino-nucleus interactions

C. Juszczak, J.A. Nowak[a], J.T. Sobczyk[*]

Institute of Theoretical Physics, Wrocław University, Pl. M. Borna 9, 50-204 Wrocław, Poland

Received: 23 July 2004 / Revised version: 8 November 2004 /
Published online: 23 December 2004 –

Abstract. We have analyzed the consequences of introducing the local density approximation combined with an effective nuclear momentum-dependent potential into the CC quasi-elastic neutrino-nucleus scattering. We note that the distribution of recoil nucleons momenta becomes smooth for low momentum values and the sharp threshold is removed. Our results may be relevant for Sci-Fi detector analysis of K2K experiments. The total amount of observed recoil protons is reduced because some of them remain bound inside the nucleus. We compare theoretical predictions for a probability of such events with the results given by NUX+FLUKA MC simulations.

1 Introduction

In recent years there has been a growing interest in the studies of neutrino interactions at energies of a few GeV [1]. It was motivated by the need for more precise measurements of neutrino oscillation parameters (θ_{13} in particular). This entails deriving the best description of interactions with free nucleons, and then incorporating nuclear effects. From the point of view of the Monte Carlo codes most (or all) nuclear effects are described with numerical packages [2] but it is enlightening how many of these effects can be presented in an analytical form.

We investigated the process $\nu_\mu\ n \to \mu^-\ p$ with the target neutron bound inside the nucleus. Computations of nuclear effects were based on the Fermi gas model which is known to work quite well in the above mentioned energy region [3]. But this approach is not completely satisfactory. For example its simple implementation leads to the conclusion that the ejected nucleons must have momenta higher than the Fermi momentum k_F [4]. However there is no physical reason why lower values of the momenta should be forbidden.

A possible solution to this problem is to introduce the local density approximation (LDA) [5]. In fact the density of nuclear matter is not constant, and accordingly it is possible to introduce the concept of a local Fermi momentum $k_F(r)$. Since the interaction can take place in a region where the Fermi momentum is arbitrarily low, the distribution of the recoil nucleons momenta becomes smoother.

Another way out of the problem can be based on a different effect. The target and the recoil nucleons are not free but they are bound inside the nucleus. The binding energy is smaller then the typical values of energy transfer but it may cause interesting effects. In this paper we consider the effective momentum-dependent optical potential and investigate how it changes distribution of the recoil nucleons momenta .

A momentum dependent potential can be obtained even from the simplest versions of the nuclear mean field theory [6]. In the covariant approach based on the Dirac equation, one has to distinguish the contributions from the scalar and vector components of the nucleon self-energy in nuclear matter. In this framework the electron-nuclei scattering was discussed in [7] with mean fields taken from [8]. More recent results on the self-energy can be found e.g. in [9] where the G-matrix approach was used. Our investigation is based on the computations presented in [10]. This choice was dictated by two reasons. Firstly, we were able to reproduce an explicit formula for the potential as a function of density (local Fermi momentum) and nucleon momentum. Secondly, we wanted to make comparisons with the numerical results of other authors who used the same potential [11] [12].

The potential used in our paper was applied in the analysis of the quasi-elastic electron-nucleus scattering with incident energy of 500 MeV and the agreement with experimental data was very good [11]. In the original paper [10] several comparisons with the nuclear physics data and with other approaches were done and a general conclusion can be drown that the optical potential was calculated with the accuracy of about 5%.

We wanted to describe both local density and potential effects simultaneously and for that we needed an analyt-

[a] e-mail: janow@ift.uni.wroc.pl

[*] J.T. Sobczyk was supported by KBN grant 105/E-344/SPB/ICARUS/P-03/DZ211/2003–2005; C. Juszczak and J.A. Nowak were supported by LNGS-TARI P10/02

ical form of the potential. We obtained a simple formula for the potential as a function of two variables: the Fermi momentum and the nucleon momentum. We incorporated this potential into our Monte Carlo generator of events and obtained a spectrum of the momenta of ejected nucleons. The simulations were performed for three nuclei: oxygen, iron and argon as these are possible targets in the neutrino experiments. The results in all three cases were very similar because the shapes and the density profiles did not differ significantly.

We investigated also the possibility that the effective potential leads to the reduction of the number of events with a nucleon ejected from the nucleus. We computed the fraction of the total cross section with an excited nucleus and no ejected nucleon in the final state. The same effect is predicted by other MC generators (e.g. NUX+FLUKA).

We have also looked for the effects related to the proton-neutron asymmetry inside the nucleus but the introduction of separate values of the Fermi momentum for proton and neutron gases left all the plots virtually unchanged.

Our results can be useful in the near detector analysis of the neutrino interaction events in the K2K where the Sci-Fi detector registers tracks of the ejected protons. The reconstruction procedure requires a particle to cross at least three planes of scintillating fiber leaving out the protons with momenta below 500 MeV. Therefore in the data analysis, it is important to have a MC generator which correctly reproduces the shape of the recoil proton momentum distribution.

We performed the MC simulations assuming the neutrino energy profile as expected at the Sci-Fi detector [13]. We investigated to what extent the spectrum of the recoil protons momenta is influenced by the simultaneous introduction of the LDA and the effective potential.

The introduction of the effective potential changes the four-momentum of the ejected nucleons and can be understood as equivalent to including some final state interactions (FSI) [14]. It is known that the resulting effects are negligible for neutrinos with energy above 5 GeV but are important for lower energies [15]. The FSI modifies the shape of the energy transfer distribution: for $E_\nu = 1\,\mathrm{GeV}$ the quasi-elastic peak is reduced by about 25% and higher values of the energy transfer become accessible [15]. For $E_\nu = 700\,\mathrm{MeV}$ the shape of the energy transfer distribution in our simulations (see Fig. 9) is modified in a similar way. It is clear that a part of what is called the FSI effects is contained in our model but further study in this direction is required.

The spectrum of the momenta of the ejected nucleons was usually studied in the context of the NC reactions where it is the only observable. The outgoing nucleons with momentum above the Cherenkov threshold for SK i.e. bigger than about 1.07 GeV were investigated recently in [16]. In an earlier study [17] an average binding energy was used to describe kinematics of the process and interesting predictions for the angular distributions of recoil nucleons were proposed. The Pauli blocking was not imposed and consequently arbitrarily low values of the momenta of the ejected nucleons were possible. Another approach [18] used Pauli blocking and accordingly forbode recoil nucleons of kinetic energy below about 27 MeV. It seems clear that any realistic model of interaction should incorporate the Pauli blocking and also a mechanism to remove the nonphysical threshold in the ejected nucleon momentum spectrum.

2 Model

Our Monte Carlo generator simulates quasi-elastic neutrino interactions with basic dynamics introduced according to [19].

The events are obtained in the following manner:

- The neutrino energy E_ν is chosen as either a fixed value or generated according to some beam energy profile.
- The Fermi momentum is established using global or local Fermi momentum scheme:
  - In the global scheme the Fermi momentum is fixed.
  - In the local scheme the region in the nucleus where the interaction is going to take place is selected first. Then the local Fermi momentum is calculated based on the nuclear density in this region.

  The actual target momentum is chosen at random from the Fermi ball of that radius.
- The nucleon neutrino pair is boosted to its center of mass frame (CMS) where the direction of the scattering is taken to be random but it will be weighted later on.
- While keeping this direction fixed in the CMS frame various values of the outgoing nucleon momentum are tested and by means of the bisection algorithm the value which brings about the energy conservation is chosen. The energy is always evaluated in the LAB frame and takes into account the momentum dependent potential of the nucleon.
- The outgoing nucleon is Pauli blocked if its momentum in the lab is smaller than the local Fermi momentum.
- The exit of the nucleon from the nuclear matter is simulated by diminishing the values of its momentum from the above calculated value p_N (inside nucleus) to the value p' (outside nucleus) calculated from the energy conservation condition

$$V(p_N) + E_k(p_N) = E_k(p') \tag{1}$$

  If there is no solution then the nucleon cannot leave the nucleus and there is only the excited nucleus in the final state. The justification for this equation comes from the fact that there is no nuclear potential outside the nucleus.
- The value of the cross section is calculated according to neutrino energy in the target rest frame. A correction of little significance (less than 1 % effect on the cross section) due to nonlinearity of the neutrino and target nucleon momenta is taken into account. The weight of the event is proportional to the nuclear density, differential cross section (with correction), the boost jacobian, the bisection algorithm jacobian.

The target is treated as a collection of nucleons distributed in space according to the density profile determined in the electron-nucleus scattering experiments. For

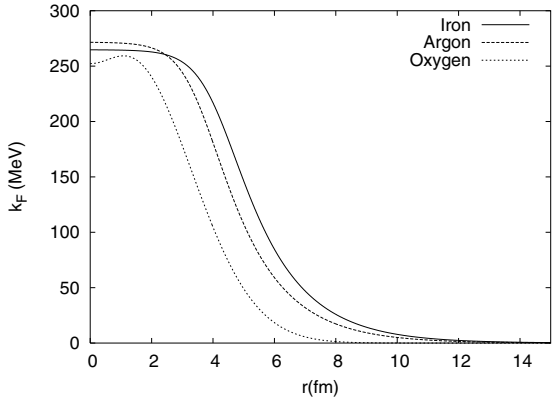

Fig. 1. The local Fermi momentum $k_F(r)$ dependence for ${}_8O^{16}$, ${}_{18}\mathrm{Ar}^{40}$ and ${}_{26}\mathrm{Fe}^{56}$

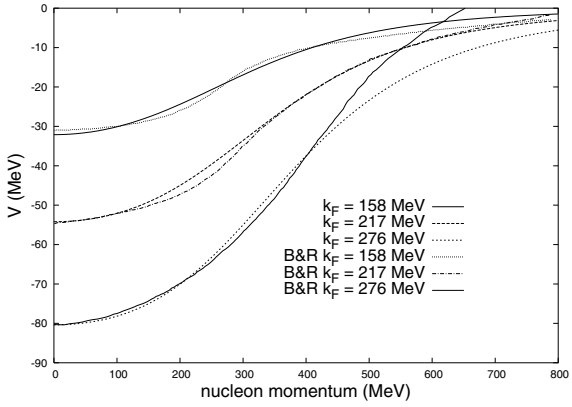

Fig. 2. The Momentum dependent potential $V(k_F, p)$ for 3 values of Fermi momentum (see (8)) compared with original plots, labeled B&R taken from [11]

the ${}_8O^{16}$ nucleus we adopted the harmonic oscillator model in which the nuclear density is given by [20]:

$$\rho^{\mathrm{O}^{16}}(r) = \rho_0 \exp\left(-r^2/R^2\right)\left(1 + C\frac{r^2}{R^2}\right) \qquad (2)$$

where $R = 1.883\,\mathrm{fm}$, $\rho_0 = 0.141\,\mathrm{fm}^{-3}$, $C = 1.544$, and ρ_0 is the normalization constant defined by the condition:

$$\int d^3r \rho^{\mathrm{O}^{16}}(r) = A\,. \qquad (3)$$

For the ${}_{18}\mathrm{Ar}^{40}$ and ${}_{26}\mathrm{Fe}^{56}$ nuclei we use the two parameter Fermi model and write the density as:

$$\rho^{\mathrm{Ar,Fe}}(r) = \frac{\rho_0}{1 + \exp\left(\frac{r-C}{C_1}\right)} \qquad (4)$$

with the following parameters:

	$\rho_0[\mathrm{fm}^{-3}]$	$C[\mathrm{fm}]$	$C_1[\mathrm{fm}]$
${}_{18}\mathrm{Ar}^{40}$	0.176	3.530	0.541
${}_{26}\mathrm{Fe}^{56}$	0.163	4.111	0.558

The local Fermi momentum is determined by the density profile according to:

$$k_F(r) = \sqrt[3]{\frac{3\pi^2\rho(r)}{2}} \qquad (5)$$

In Fig. 1 we show the local Fermi momentum dependence on r in Oxygen, Argon and Iron nuclei. In the case of non-symmetric nuclei one can also introduce separate local Fermi momenta for protons and neutrons:

$$k_F^p(r) = \sqrt[3]{\frac{2Z}{A}}k_F(r), \qquad k_F^n(r) = \sqrt[3]{\frac{2N}{A}}k_F(r)\,. \qquad (6)$$

where A, Z, and N are the atomic number, the number of protons, and the number of neutrons in the nucleus, respectively.

Defining the average value of k_F as:

$$\left\langle k_F^{\mathrm{nucleus}}\right\rangle = \frac{\int k_F(r)\, r^2 \rho^{\mathrm{nucleus}}(r)\, dr}{\int r^2 \rho^{\mathrm{nucleus}}(r)\, dr}\,, \qquad (7)$$

we get the following values:

$$\langle k_F^{\mathrm{O}}\rangle = 199\,\mathrm{MeV}\,,$$
$$\langle k_F^{\mathrm{Ar}}\rangle = 217\,\mathrm{MeV}\,,$$
$$\langle k_F^{\mathrm{Fe}}\rangle = 217\,\mathrm{MeV}\,.$$

Using the results from [10] we fit the real part of the optical potential with the formula (see Fig. 2):

$$V(k_F, p) = -\frac{(ak_F)^2(k_F + b)}{c^4 + d^3k_f + e^3p^2/k_f + p^4}\,, \qquad (8)$$

where k_F, p, and $V(k_F, p)$ are given in MeV and the values of the parameters are:
$a = 206\,\mathrm{MeV}$, $b = 582\,\mathrm{MeV}$, $c = -322\,\mathrm{MeV}$, $d = 422\,\mathrm{MeV}$, and $e = 289\,\mathrm{MeV}$.

The form (8) of the potential fulfills the following criteria:

- V is negative,
- V reproduces the essential features of the plots from [10],
- V is monotonously increasing,
- For higher values of the momentum, V quickly approaches zero,
- For small values of the momentum, V is proportional to p^2 as in the limit as $p \to 0$ one expects on general grounds that

$$V(p) + \frac{p^2}{2M} \sim V_0 + \frac{p^2}{2M^*}\,, \qquad (9)$$

where $M^* < M$ is an effective nucleon mass. There is some amount of uncertainty in the reconstructed potential which is inherited from the original computations in which contributions from only a finite number ($L \leq 4$) of harmonics were included.

3 Results

In the numerical computations we compare three cases:

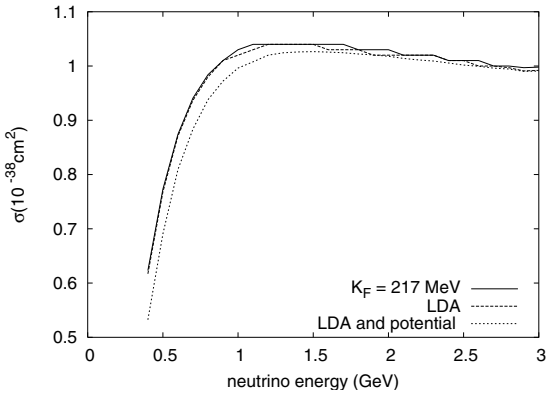

Fig. 3. Total cross section (per nucleon) for quasi-elastic scattering on iron

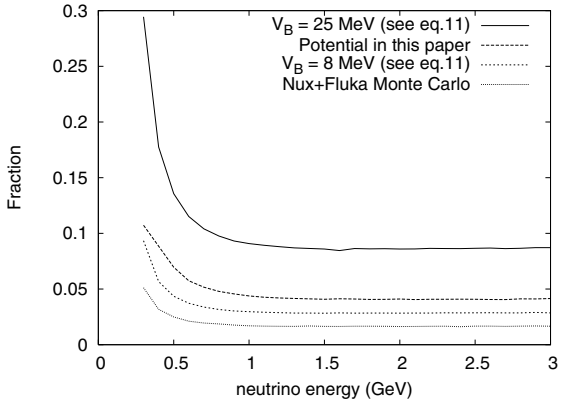

Fig. 4. A fraction of the total cross section corresponding to events in which proton remains bounded in an excited nucleus

(a) Fermi gas with global $k_F = \langle k_F^{\rm nucleus} \rangle$,
(b) Fermi gas in the local density approximation (LDA),
(c) Fermi gas in the local density approximation with momentum dependent effective potential (8).

The total cross sections for quasi-elastic interaction for all three cases are plotted in Fig. 3. While changes introduced by the LDA are minor, the inclusion of the effective potential reduces the total cross section by a few percent.

Since the recoil nucleon is affected by the momentum dependent potential it may not have enough energy to leave the nucleus. In such a case the final state consists of the excited nucleus and there is no ejected nucleon. This happens always if

$$V(p_N) + E_k(p_N) \leq \ M\,. \tag{10}$$

The probability of such a process is shown in Fig. 4. For comparison, we calculated the probability of analogous events in the NUX+FLUKA MC generator [2]. We note that the shapes of the curves are in both cases almost identical. The probability for a bound nucleon in the final state decreases with neutrino energy in both generators and becomes flat at energy of about 1 GeV. However, the probability predicted by our Monte Carlo generator is much higher (about three times) than the probability obtained from NUX+FLUKA (see Fig. 4).

We tried to understand this discrepancy by considering a very simple model in which the nucleons are subject to the potential

$$E_F + V_B\,, \tag{11}$$

where E_F is the Fermi energy and V_B is the binding energy [2]. Performing the simulations for several values of V_B we discovered that not only the shapes of the curves were similar to those obtained in more sophisticated models but, it was also possible to mimic both NUX+FLUKA and our MC generator results by carefully choosing the values of V_B. The results of NUX+FLUKA generator which takes into account many nuclear effects were reproduced by assuming the effective value $\langle V_B \rangle_{\rm eff} \sim 5\,{\rm MeV}$ while the approach presented in this paper corresponds to $\langle V_B \rangle_{\rm eff} \sim 12\,{\rm MeV}$. In the Fig. 4 we showed the curves obtained from the simple model for $V_B = 8\,{\rm MeV}$ and $V_B = 25\,{\rm MeV}$ along with the curves obtained with the two discussed generators.

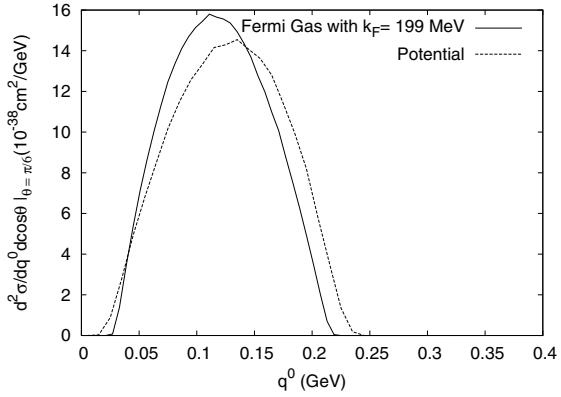

Fig. 5. Differential quasi-elastic neutrino-nucleus scattering cross section at fixed muon scattering angle $\theta_\mu = 30^o$. The incident neutrino energy is $E_\nu = 1000\,{\rm MeV}$

We verified the consistency of our computational procedures by comparing our results with those obtained by Seki and Nakamura [12]. In the comparison we did not take into account the LDA effects because they are not included in the other analysis. In Fig. 5, we present the plots of the differential cross section as a function of the energy transfer for the fixed value of the muon scattering angle $\theta_\mu = 30^o$. We compare the predictions of the Fermi gas model with $k_F = 199\,{\rm MeV}$ and the approach based on the effective potential. We note that the potential induces modifications which are very similar to those seen in Fig. 3 of [12].

The predicted distributions of the ejected nucleon momentum are shown in Fig. 6 and 7. The plots are normalized as the differential cross sections $d\sigma/dp'$ and the neutrino energy is fixed at 700 MeV. The changes introduced due to the LDA and the effective potential are very similar for all three analyzed targets so we omit the plot for iron.

In the case (a) (see the end of the Sect. 2) there are obvious sharp thresholds at $\langle k_F^{\rm nucleus} \rangle$.

In the case (b) the distributions become smoother. They differ only in the region of nucleon momentum below $\sim$ 300 MeV; whereas, for higher values of nuclear momentum, LDA introduces no significant differences.

Finally, in the case (c) there is higher probability for the outgoing nucleon to have momentum lower than k_F. The values close to zero become accessible as well. The differen-

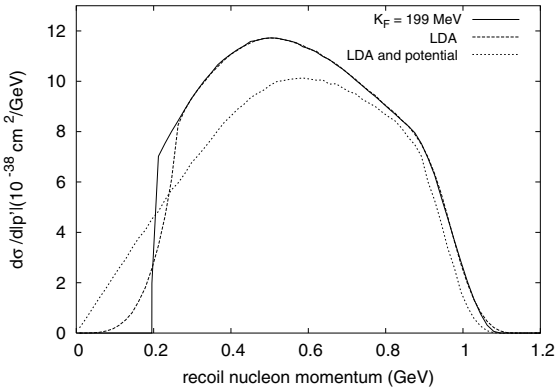

Fig. 6. Recoil nucleons momentum distribution for quasi-elastic neutrino-oxygen scattering. The incident neutrino energy is $E_\nu = 700\,\mathrm{MeV}$

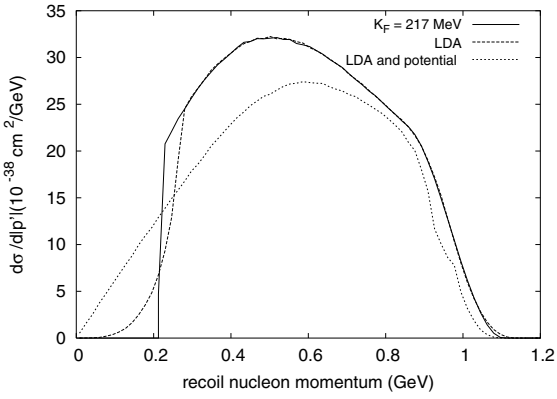

Fig. 7. Recoil nucleons momentum distribution for quasi-elastic neutrino-argon scattering. The incident neutrino energy is $E_\nu = 700\,\mathrm{MeV}$

tial cross section rises almost linearly for nucleon momenta smaller than 450 MeV than it slowly bends reaching maximum at about 600 MeV. For momenta above 800 MeV the plot is only slightly changed compared to the cases (a) and (b).

The Fig. 8 illustrates the relevance of the introduction of separate values of Fermi momentum for neutron and proton Fermi gases. The Fermi momentum for neutrons is larger and since the neutrino interaction takes place on neutrons, it is clear that the cross section should be slightly increased. It is indeed the case but the effect is very small and the difference of the plots is hardly noticeable.

For completeness in Fig. 9 we present how both discussed effects influence the energy transfer spectrum for the iron nucleus (plots for oxygen and argon are very similar). There is only a small difference at the peak between the differential cross section plots for the cases (a) and (b), the plot for the LDA being slightly lower. In the case (c) we observe a significant change in the shape. For lower values of the energy transfer the differential cross section is substantially reduced and for higher energy transfers it is increased. The allowed kinematical region is enlarged.

In Fig. 10 we show the ejected proton momentum distribution obtained for a neutrino beam with the energy profile identical to that predicted for the K2K near detector. The plot is normalized to be an effective (energy averaged) differential cross section.

We note that the LDA and the potential effects remove the sharp threshold and give a smooth plot at low values of the momentum. The number of nucleons with momentum between k_F and 700 MeV is significantly reduced but the values between 0 and k_F become possible.

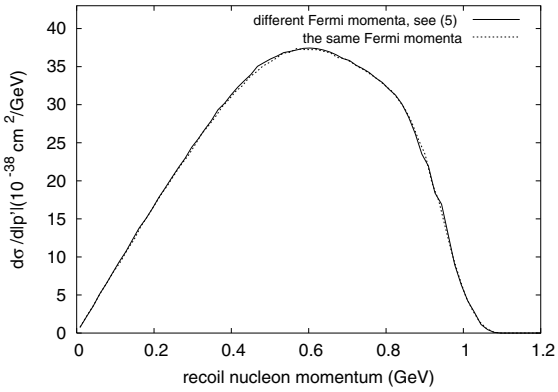

Fig. 8. The dependence of the distribution of momenta of ejected nucleons on the assumption of different values of Fermi momenta for protons and neutrons in quasi-elastic neutrino-iron scattering. The incident neutrino energy is $E_\nu = 700\,\mathrm{MeV}$

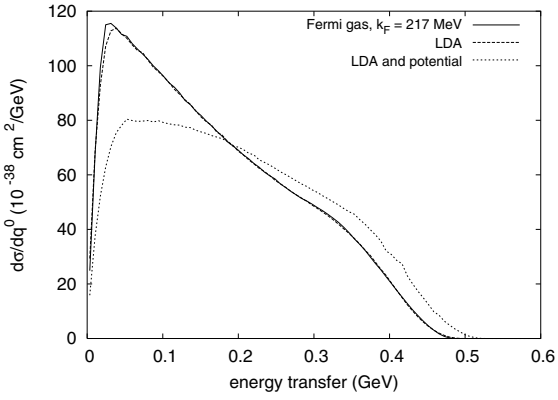

Fig. 9. Differential cross section of energy transfer for quasi-elastic neutrino-iron scattering. The incident neutrino energy is $E_\nu = 700\,\mathrm{MeV}$

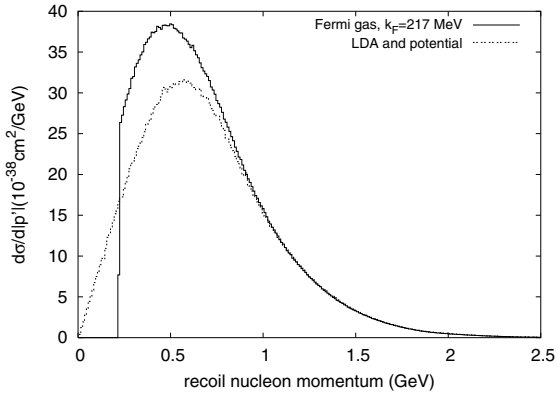

Fig. 10. The distribution of recoil nucleons in quasi-elastic reactions on iron for neutrino energy spectrum identical with that predicted at K2K near detector

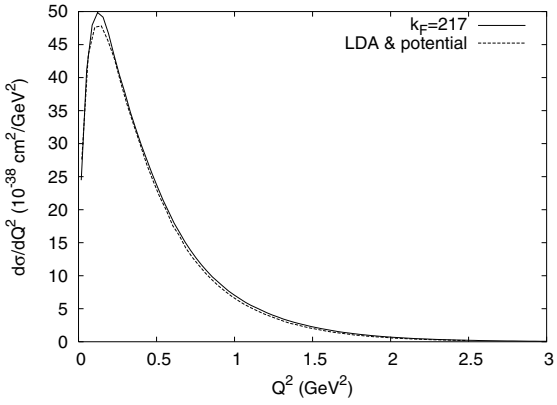

Fig. 11. Differential cross section of Q^2 transfer for quasi-elastic neutrino-iron scattering for neutrino energy spectrum identical with that predicted at K2K near detector

With LDA and potential effects there is a probability of about 4% that the nucleon remains bounded inside nucleus and the area below the corresponding curve is accordingly reduced.

In Fig. 11 we show the momentum transfer distribution for quasi-elastic events produced with the same K2K-like beam. It is clear that it is insensitive to the effects discussed in the present paper.

References

1. J.G. Morfin, M. Sakuda, Y. Suzuki (eds.), Proceedings of the First International Workshop on Neutrino-Nucleus Interactions in the Few GeV Region, Nucl. Phys. B (Proc. Suppl.) **112** (2002) November 2002; for talks on NuInt02 Workshops see http://nuint.ps.uci.edu/
2. G. Battistoni, A. Ferrari, A. Rubbia, P.R. Sala, The FLUKA nuclear cascade model applied to neutrino interactions, to appear in Proc. of NUINT 2002; see http://nuint.ps.uci.edu/
3. R.A. Smith, E.J. Moniz, Nucl. Phys. B **43**, 605 (1972)
4. C.W. Walter, Nucl. Phys. B (Proc. Suppl.) **112**, 140 (2002)
5. S.K. Singh, E. Oset, Phys. Rev. C **48**, 1246 (1993); T.S. Kosmas, E. Oset, Phys. Rev. C **53**, 1409 (1996)
6. B.D. Serot, J.D. Walecka, Adv. Nucl. Phys. **16**, 1 (1986)
7. H. Kim, C.J. Horowitz, M.R. Frank, Phys. Rev. C **51**, 792 (1995)
8. E.D. Cooper, S. Hama, B.C. Clark, R.L. Mercer, Phys. Rev. C **47**, 297 (1993)
9. E. Schiller, H. Müther, Eur. Phys. J. A **11**, 15 (2001)
10. F.A. Brieva, J.R. Rook, Nucl. Phys. A **291**, 299 (1977)
11. F.A. Brieva, A. Dellafiore, Nucl. Phys. A **292**, 445 (1977);
12. H. Nakamura, R. Seki, Nucl. Phys. B (Proc. Suppl.) **112**, 197 (2002)
13. S.H. Ahn, et al. (K2K collaboration), Phys.Lett. B **511**, 178 (2001)
14. D.B. Day, J.S. McCarthy, T.W. Donnelly, I. Sick, Ann. Rev. Nucl. Part. Sci. **40**, 357 (1990)
15. G. Co', C. Bleve, I. De Mitri, D. Martello, Nucl. Phys. B (Proc. Suppl.) **112**, 210 (2002); C. Bleve, G. Co', I. De Mitri, P. Bernardini, G. Mancarella, D. Martello, A. Surdo, Astropart. Phys. **16**, 145 (2001)
16. J.F. Beacom, S. Palomares-Ruiz, Phys. Rev. D **67**, 093001 (2003)
17. C.J. Horowitz, H. Kim, D.P. Murdock, S. Pollock, Phys. Rev. C **48**, 3078 (1993)
18. W.M. Alberico, M.B. Barbaro, Samoil M. Bilenky, J.A. Caballero, C. Giunti, C. Maieron, E. Moya de Guerra, J.M. Udias, Nucl. Phys. A **623**, 471 (1997)
19. C.H. Llewellyn Smith, Phys. Rep **3**(5), 261 (1972)
20. H. De Vries, C.W. de Jager, C. De Vries, Atomic Data and Nuclear Tables, **36**, 495 (1987)